Numerical Simulation of Extrusion Casting Based on SPH Method

Yuwei Cui[1], Ruiqi Li[1], Yue Pan[3], Xiaofeng Niu[4], Liwen Chen[1], Yuhong Zhao[1,2,5,*]

1. School of Materials Science and Engineering, MOE jointly Collaborative Innovation Center for High-performance Al/Mg based Materials, Shanxi Key Laboratory of Intelligent Casting and Advanced Forming for New Materials, Taiyuan, 030051, China ;
2. Beijing Advanced Innovation Center for Materials Genome Engineering, University of Science and Technology Beijing, Beijing, 100083, China ;
3. School of Materials Science and Engineering, Taiyuan University of Science and Technology, Taiyuan, 030024, China ;
4. College of Materials Science and Engineering,Taiyuan University of Technology, Taiyuan, 030000, China ;
5. Institute of Materials Intelligent Technology, Liaoning Academy of Materials, Shenyang, 110004, China.

*Corresponding address: e-mail: zhaoyuhong@nuc.edu.cn

Abstract: The traditional grid-based casting numerical simulation method often experiences grid overlap, distortion and entanglement when dealing with free surface problems and local deformation problems of fluids, thereby reducing the accuracy of numerical simulation. For this purpose, this paper independently developed a simulation casting calculation program based on Smooth particle fluid Dynamics (SPH), and conducted numerical simulation studies on the filling and solidification processes of extrusion casting. The simulation results were compared and verified with the foreign casting numerical simulation software ProCAST to provide assistance for the SPH method in simulating and predicting casting filling and formulating actual production process parameters.

Keywords: Smoothed Particle Hydrodynamics; Squeeze Casting; Numerical Simulation

1 Introduction

Squeeze casting [1,2] is a near-net-shape material forming technology that combines the processes of forging and casting. With its advantages such as high productivity, high precision, and material savings, it has gained significant popularity in the production of high-performance metal structural components. Traditional casting technology not only requires repeated trials but also consumes a large amount of human and material resources, which has hindered the progress of China's industrial modernization. With the development of computers and related sciences, the application of computer simulation technology in casting forming has received increasing attention, and numerical simulation technology [3-7] has also been widely applied in the squeeze casting industry. Since the 1980s, the numerical simulation technology of squeeze casting has been continuously evolving and has achieved remarkable achievements both at home and abroad. Traditional casting numerical simulation mainly relies on the Finite Element Method [8,9], the Finite Difference Method [10,11], and the Finite Volume Method [12-14] for numerical calculations. For example, XU Ruo-zhen et al.[15] conducted a numerical simulation analysis of the squeeze casting process of an automobile subframe using ProCAST software, providing a theoretical basis for determining the squeeze casting process plan. LI et al.[16] carried out a numerical simulation analysis of the squeeze casting process of an automobile control arm using Magma software. Through numerical simulation, they accurately predicted the location of solidification defects, providing strong support for optimizing the casting process. BABAEE et al.[17] simulated the squeeze casting process of Al/Al-4.5%Cu (mass fraction) bimetal using ProCAST and Ansys software. The simulation results showed that a relatively large stress appeared at the interface of the bimetal. CheneyL et al.[18] established a three-dimensional mathematical calculation model for the rapid coupling of heat flow and pressure between the squeeze-cast aluminum alloy part and the slurry through numerical analysis, and carried out a three-dimensional

numerical simulation using the finite volume method. The numerical simulation results were consistent with the experimental results, further verifying the reliability of the model. The EasyCast casting simulation software developed by North University of China[19] proposed a grid meshing method for casting simulation based on boundary grid projection. When applied to complex castings with inclined surfaces and arc surfaces, this method effectively avoids the loss of the inclination information of the castings, thereby improving the accuracy of subsequent casting numerical simulations. Although traditional grid-based casting numerical simulation methods have been widely used in the casting process, grid overlapping, distortion, and entanglement often occur when dealing with free surface fluid problems and local deformation problems of fluids, which in turn reduces the accuracy of numerical simulations. To overcome the disadvantages and limitations of the grid method, the meshless method came into being. The Smoothed Particle Hydrodynamics (SPH) method [20-22] is one of the most widely used and rapidly developing meshless methods. It describes a continuous medium using a group of interacting particles, with various physical quantities carried by each particle. By solving the dynamic equations of the particle group and tracking the motion trajectory of each particle, the mechanical behavior of the entire system can be obtained. The SPH method was first proposed by LUCY [23] and GINGOLD et al. [24] in 1977 to solve astrophysical problems in three-dimensional open space. Cleary et al. [25-27] used the SPH method to numerically simulate the high-pressure and low-pressure casting processes, and the results were in good agreement with the experiments in the casting verification studies. Ha et al.[28] also demonstrated that the SPH method can predict the filling process in gravity casting, proving its application potential in gravity casting. Colagrossia et al.[29] studied the application of the SPH method in dealing with gas-liquid two-phase flow problems, and calculated the problems of bubble rising in liquid and the gas-liquid two-phase flow during the dam break process. JIA Jinbo et al. [30] used the SPH method to predict the cold shut defects of castings; SHEN Mengqing et al.[31] carried out a numerical simulation study of the selective laser melting process of 316L stainless steel powder using the SPH method. The SPH method has properties such as meshlessness, self-adaptability, stability, and Lagrangian characteristics, and it has received increasing attention, providing a new approach and method for casting numerical simulation technology.

Based on the above, this paper independently developed a calculation program for simulating the casting process based on the SPH method, and conducted a numerical simulation study on the filling process of squeeze casting. The simulation results were compared and verified with the foreign casting numerical simulation software ProCAST, aiming to provide assistance for the SPH method in simulating and predicting the filling of castings and formulating actual production process parameters.

2 Establishment of the SPH Flow Field Model

2.1 Basic Equations of the SPH Method

In the SPH method, first, continuous physical quantities are approximately transformed into integral expressions through kernel functions to achieve the calculation of weighted averages of field variables and their gradients in space. Then, the particle approximation method is adopted to discretize the continuous integral expression, and then the numerical calculation of the field variable is achieved through the discrete summation of adjacent particles Suppose $f(x)$ is a continuous and smooth function defined on the region Ω, and its function value at any point can be expressed by the SPH method as:

$$f(x) = \int_{\Omega} f(x')\delta(x - x')\mathrm{d}x' \#(1)$$

where $\delta(x - x')$ is the Dirac function, and x is the position vector in space. The Dirac function has specific mathematical properties, and its definition is:

$$\delta(\boldsymbol{x} - \boldsymbol{x}') = \begin{cases} 1, & \boldsymbol{x} = \boldsymbol{x}' \\ 0, & \boldsymbol{x} \neq \boldsymbol{x}' \end{cases} \#(2)$$

In practical calculations, it is difficult to represent the Dirac function accurately. Therefore, a smooth kernel function $W(\boldsymbol{x} - \boldsymbol{x}', \mathrm{h})$ is often used to replace the Dirac function to improve the calculation stability:

$$f(x) \approx \int_{\Omega} f(x')W(\boldsymbol{x} - \boldsymbol{x}', h)d\boldsymbol{x}' \#(3)$$

where the value of the smooth kernel function $W(\boldsymbol{x} - \boldsymbol{x}', \mathrm{h})$ depends on the smoothing length $\boldsymbol{h}$ and the distance $\boldsymbol{x} - \boldsymbol{x}'$ between particles. To ensure the accuracy of numerical calculations, the kernel function must satisfy four conditions: normalization, compact support, even function property, and consistency with the Dirac function.

In the above formula, κ is a proportionality factor, and κh determines the size of the influence domain of the local smooth function.

Through the kernel approximation method, equation (3) can be rewritten as:

$$\langle f(\boldsymbol{x})\rangle = \int_{\Omega} f(\boldsymbol{x}')W(\boldsymbol{x}-\boldsymbol{x}',h)d\boldsymbol{x}' \#(4)$$

Replace $f(\boldsymbol{x})$ with the spatial derivative $\boldsymbol{\nabla}\cdot f(\boldsymbol{x})$ to obtain the following description:

$$\langle \boldsymbol{\nabla}\cdot f(\boldsymbol{x})\rangle = \int_{\Omega} [\boldsymbol{\nabla}\cdot f(\boldsymbol{x}')]\, W(\boldsymbol{x}-\boldsymbol{x}',h)d\boldsymbol{x}' \#(5)$$

After adjusting the coordinate system according to the above equation, the following form is obtained:

$$\langle \boldsymbol{\nabla}\cdot f(\boldsymbol{x})\rangle = \int_{\Omega} \nabla\cdot f(\boldsymbol{x}')W(\boldsymbol{x}-\boldsymbol{x}',h)d\boldsymbol{x}' - \int_{\Omega} f(\boldsymbol{x}')\cdot\nabla W(\boldsymbol{x}-\boldsymbol{x}',h)d\boldsymbol{x}' \#(6)$$

When applying the divergence theorem to the first term on the right - hand side of the above equation, the following formula can be derived:

$$\langle \boldsymbol{\nabla}\cdot f(\boldsymbol{x})\rangle = \int_{S} f(\boldsymbol{x}')W(\boldsymbol{x}-\boldsymbol{x}',h)\cdot\vec{n}dS - \int_{\Omega} f(x')\cdot\boldsymbol{\nabla}W(\boldsymbol{x}-\boldsymbol{x}',h)d\boldsymbol{x}' \#(10)$$

where $\vec{n}$ is the unit normal vector of the surface region S.

After simplification, it can be expressed by (7):

$$\langle \boldsymbol{\nabla}\cdot f(\boldsymbol{x})\rangle = -\int_{\Omega} f(\boldsymbol{x}')\cdot\nabla W(\boldsymbol{x}-\boldsymbol{x}',h)d\boldsymbol{x}' \#(7)$$

A crucial issue in the SPH method is how to select an appropriate smooth kernel function to ensure accurate approximation of arbitrarily distributed discrete points. The choice of the smooth function not only determines the size of the particle region but also affects the accuracy and consistency of the kernel approximation. Common smooth kernel functions include the cubic spline smooth function [32,33], Gaussian function[34], bell - shaped function[35], and quartic function[36], etc. In this paper, the cubic spline smooth function is adopted, which has good smoothness and stability between continuous points. Its definition is as follows:

$$W(R,h) = \alpha_d \begin{cases} \frac{2}{3} - R^2 + \frac{1}{2}R^3, & 0 \le \mathrm{R} \le 1; \\ \frac{1}{6}(2-R)^3, & 1 < \mathrm{R} < 2; \\ 0, & \mathrm{R} \ge 2 。 \end{cases} \#(8)$$

When the dimension is one - dimensional, $\alpha_d = \frac{1}{\mathrm{h}}$; when the dimension is two - dimensional, $\alpha_d = \frac{5}{7\pi \mathrm{h}^2}$; when the dimension is three - dimensional, $\alpha_d = \frac{3}{2\pi \mathrm{h}^3}$. Here, the relative distance R is calculated by the formula $R = \frac{\mathrm{r}}{\mathrm{h}} = \frac{|x-x'|}{\mathrm{h}}$, where r represents the actual distance between two particles, and h is the smoothing length.

The particle approximation method discretizes the field of the continuous medium into particles with physical properties, and then combines these particles through approximate calculations to construct the numerical solution of the support domain. Figure 2 shows the core idea of the particle approximation method, where the center of particle i and its radius κh form the support region of the kernel function W in the domain Ω.

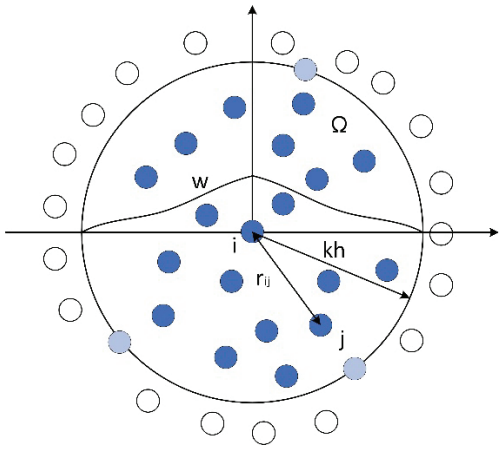

Fig. 1 A sketch of the core idea of the particle approximation method

Suppose the volume ΔV_j of particle j can be regarded as an approximation of the infinitesimal difference of the integral dx, and the mass m_j of particle j can be expressed as:

$$m_j = \rho_j \Delta V_j \#(9)$$

where ρ_j is the density of particle j ($j = 1, 2, 3, \ldots\ldots, N$), and N represents the total number of particles in the support domain.

Discretize the SPH integral formula in equation (10) to obtain the discrete form of the particle approximation:

$$f(\boldsymbol{x}) \approx \sum_{j=1}^{N} f(\boldsymbol{x}_j)\mathrm{W}(\boldsymbol{x}-\boldsymbol{x}',h)\,\Delta V_j = \sum_{j=1}^{N} f(\boldsymbol{x}_j)\mathrm{W}(\boldsymbol{x}-\boldsymbol{x}',h)\frac{m_j}{\rho_j} \#(11)$$

Therefore, the final field function at particle i can be approximately written as:

$$\langle f(\boldsymbol{x}_i)\rangle = \sum_{j=1}^{N} \frac{m_j}{\rho_j} f(\boldsymbol{x}_j) W_{ij} \#(12)$$

where W_{ij} is the kernel function between particle i and particle j:

$$W_{ij} = W(\boldsymbol{x}_i - \boldsymbol{x}_j, h) \#(13)$$

The formula for calculating the spatial derivative of the function using the particle approximation method is as follows:

$$\langle \nabla \cdot f(\boldsymbol{x}_j)\rangle = -\sum_{j=1}^{N} \frac{m_j}{\rho_j} f(\boldsymbol{x}_j) \cdot \nabla W(\boldsymbol{x}_i - \boldsymbol{x}_j, h) \#(14)$$

The gradient of the kernel function ∇W_{ij} can be calculated by the following formula:

$$\nabla W_{ij}(\boldsymbol{x}_i - \boldsymbol{x}_j, h) = \frac{x_i - \boldsymbol{x}_j}{r_{ij}} \frac{\partial W_{ij}}{\partial r_{ij}} \#(15)$$

where r_{ij} is the distance between particle i and particle j.

Continuously applying formula (14) can calculate the derivative of the field function, and through further processing, more accurate calculation results can be obtained. Through integration by parts, the following expressions are obtained:

$$\nabla \cdot f(\boldsymbol{x}) = \frac{1}{\rho}\left[\nabla \cdot (f(\boldsymbol{x})\rho) - f(\boldsymbol{x}) \cdot \nabla \rho\right] \#(16)$$

or

$$\nabla \cdot f(\boldsymbol{x}) = \rho\left[\nabla \cdot \left(\frac{f(\boldsymbol{x})}{\rho}\right) + \frac{f(\boldsymbol{x})}{\rho^2} \cdot \nabla \rho\right] \#(17)$$

Apply formula (14) to formulas (16) and (17), and the approximate derivative of the field function at the position of particle i can be obtained as:

$$\langle \nabla \cdot f(\boldsymbol{x}_i)\rangle = \frac{1}{\rho_i} \sum_{j=1}^{N} m_j \left[f(\boldsymbol{x}_j) - f(\boldsymbol{x}_i)\right] \cdot \nabla_i W_{ij} \#(18)$$

$$\langle \nabla \cdot f(\boldsymbol{x}_i)\rangle = \rho_i \sum_{j=1}^{N} m_j \left[\frac{f(\boldsymbol{x}_j)}{\rho_j^2} + \frac{f(\boldsymbol{x}_i)}{\rho_i^2}\right] \cdot \nabla_i W_{ij} \#(19)$$

2.2 Navier-Stokes Equations Based on the SPH Method

The basic governing equations of fluid mechanics are derived from three fundamental physical conservation laws: mass conservation, momentum conservation, and energy conservation. This series of equations is known as the Navier-Stokes equations [37,38], and the Lagrangian form of the expressions is as follows:

For the mass conservation equation, the expression of the mass conservation equation is:

$$\frac{d\rho}{dt} = -\rho \nabla \cdot v \#(20)$$

$\frac{d}{d_t}$ is the material derivative, ρ represents the density, and $\nabla \cdot v$ is the velocity divergence.

In the process of solving the mass conservation equation using SPH, the above - mentioned smooth kernel function approximation and particle approximation methods are required to discretize and solve the equation. For the mass conservation equation, first, the continuous density method is used to sum all particles, and then the SPH approximation is performed. Thus, the SPH expression of the mass conservation equation is obtained as:

$$\frac{d\rho_i}{dt} = \sum_{j=1}^{N} m_j v_{ij} \cdot \nabla_i W_{ij} \#(21)$$

where the expression of the continuous density method is:

$$\rho_i = \sum_{j=1}^{N} m_j W_{ij} \#(22)$$

In the formula, N represents the number of neighboring particles of the central particle i, m_j represents the mass of particle j, W_{ij} represents the smooth function effect of particle j on the central particle i, and the relative velocity $v_{ij} = v_i - v_j$.

For the momentum conservation equation, without considering the influence of surface tension and heat conduction on the equation, the standard form of the momentum equation is:

$$\frac{dv}{dt} = -\frac{1}{\rho}\nabla p + \frac{\eta}{\rho}\nabla^2 v + F \#(23)$$

where $-\frac{1}{\rho}\nabla p$ is the pressure gradient term, ρ is the density, p is the hydrostatic pressure, $\frac{\eta}{\rho}\nabla^2 v$ is the viscous term, η is the kinematic viscosity coefficient, v represents the velocity of the fluid, and the third term F is the external force term, which is the sum of gravity, punch pressure, and surface tension.

In the SPH method, the discretization treatment of the momentum equation is as follows. First, the pressure gradient term is discretized as:

$$-\frac{1}{\rho}\nabla p = -\sum_{j=1}^{N} m_j \left(\frac{p_i}{\rho_i^2} + \frac{p_j}{\rho_j^2}\right) \nabla_i W_{ij} \#(24)$$

Secondly, the discretization expression of the viscous term is:

$$\frac{\eta}{\rho}\nabla^2 v=\sum_{j=1}^{N} m_j\frac{\eta_i+\eta_i}{\rho_i\rho_j}v_{ij}\left(\frac{1}{r_{ij}}\frac{\partial W_{ij}}{\partial r_{ij}}\right)\#(25)$$

where r_{ij} is the distance between particle i and particle j. Finally, the discretized form of the momentum conservation equation can be written as:

$$\frac{dv_i}{dt}=-\sum_{j=1}^{N} m_j\left(\frac{p_i}{\rho_i^2}+\frac{p_j}{\rho_j^2}\right)\nabla_i W_{ij}+\sum_{j=1}^{N} m_j\frac{\eta_i+\eta_i}{\rho_i\rho_j}v_{ij}\left(\frac{1}{r_{ij}}\frac{\partial W_{ij}}{\partial r_{ij}}\right)+F\#(26)$$

According to the law of energy conservation, the basic form of the energy equation is:

$$\frac{\mathrm{d}e}{dt}=\frac{\sigma}{\rho}\nabla\cdot\boldsymbol{v}\#(27)$$

where e is the fluid energy and σ is the total stress tensor. The discretized form of the energy equation under the SPH method is:

$$\frac{\mathrm{d}e_i}{dt}=\frac{1}{2}\sum_{j=1}^{N} m_j\frac{\mathrm{P}_i+\mathrm{P}_j}{\rho_i\rho_j}\boldsymbol{v}_{ij}\frac{\partial \mathrm{W}_{ij}}{\partial r_{ij}}\#(28)$$

where P is the pressure, $\boldsymbol{v}_{ij}$ is the relative velocity, W_{ij} is the value of the smooth kernel function, and $\frac{\partial \mathrm{W}_{ij}}{\partial r_{ij}}$ is the derivative of the kernel function with respect to the particle spacing. In summary, the SPH method can discretize the mass, momentum, and energy conservation equations in the Navier-Stokes equations respectively, and simulate the dynamic behavior of the fluid by solving the discretized equations. This method has good numerical stability and accuracy and is widely used in the simulation of complex fluid systems.

2.3 SPH Correction Methods

When using the SPH method for calculations, in order to solve problems such as particle penetration and oscillation that may occur between particles, an artificial viscosity correction is introduced [39], and its expression is:

$$\Pi_{ij}=\begin{cases}\dfrac{-\alpha_\Pi\overline{c_{ij}}\phi_{ij}+\beta_\Pi\phi_{ij}^2}{\overline{\rho_{ij}}} & v_{ij}\cdot x_{ij}<0\\ 0 & v_{ij}\cdot x_{ij}\geq 0\end{cases}\#(29)$$

where:

$$\phi_{ij}=\frac{h_{ij}v_{ij}\bullet x_{ij}}{|x_{ij}|^2+\varphi^2}\#(30)$$

$$\overline{c}_{ij}=\frac{1}{2}(c_i+c_j)\#(31)$$

$$\overline{\rho}_{ij}=\frac{1}{2}(\rho_i+\rho_j)\#(32)$$

$$h_{ij}=\frac{1}{2}(h_i+h_j)\#(33)$$

In the formulas, a_Π and β_Π are standard parameters that control the intensity of the artificial viscosity. To prevent divergence in numerical calculations, it is usually set that $\phi=0.1\mathrm{h}_{ij}$; c is the particle sound speed, v is the particle velocity vector, and x is the particle displacement vector.

When the SPH method is used for second - order solutions, problems such as tensile instability and low - accuracy results may occur. Therefore, an artificial stress correction method is proposed: when particles approach each other, when the distance between particles is less than a certain minimum distance, a small repulsive force in the opposite direction is applied to this pair of particles to prevent the particles from getting too close and aggregating. By introducing an artificial stress correction term [40], the stability of the momentum equation can be improved, and the expression of the corrected momentum equation is:

$$\frac{dv_i}{dt}=-\sum_{j=1}^{N} m_j\left(\frac{p_i+p_j}{\rho_i\cdot\rho_j}+\Pi_{ij}+R_{ij}^{\alpha\beta}f_{ij}^n\right)\nabla_i W_{ij}+\sum_{j=1}^{N} m_j\frac{\eta_i+\eta_i}{\rho_i\rho_j}v_{ij}\left(\frac{1}{r_{ij}}\frac{\partial W_{ij}}{\partial r_{ij}}\right)+F\qquad(34)$$

where p_i, p_j are the pressures of the corresponding particles; f_{ij}^n is the correction factor of the kernel function:

$$f_{ij}^n=\frac{W(r_{ij})}{W(\Delta p)}\#(35)$$

where Δp is the initial particle spacing; R_{ij} is the mean value of two particles:

$$R_{ij}^{\alpha\beta}=\frac{1}{2}(R_{\mathrm{i}}^{\alpha\beta}+R_j^{\alpha\beta})\#(36)$$

$$R_i^{\alpha\beta}=\begin{cases}-\varepsilon_s\dfrac{\sigma_i^{\alpha\beta}}{\rho_i^2}, \sigma_i^{\alpha\beta}>0\\ 0, \sigma_i^{\alpha\beta}<0\end{cases}\#(37)$$

$$R_i^{\alpha\beta}=\begin{cases}\varepsilon_s\dfrac{|P_i|}{\rho_i^2}, P_i<0\\ 0, P_i>0\end{cases}\#(38)$$

where the value of ε_s is 0.3, which is used to adjust the influence range of the stress, and the value of n is 0.3.

The artificial compression method is a simulation method commonly used to deal with incompressible fluids. To further improve the accuracy of the calculation

results, we can handle the compressibility problem of free - surface fluids by using equations of

state such as the water equation of state. Its equation of state is as follows:

$$P = P_0\left[\left(\frac{\rho}{\rho_0}\right)^{\gamma} - 1\right]\#(39)$$

where ρ_0 is the density value in the initial state; γ is a constant, usually taken as 7 to adjust the compressibility of the fluid; P_0 is the reference pressure, which needs to be appropriately selected according to the problem in actual calculations. Its calculation method is $P_0 = \frac{c_0^2\rho_0}{\gamma}$, where c_0 is the acoustic wave velocity related to the density. Under the approximation condition of weak compressibility, the acoustic wave velocity c_0 of the fluid can reach ten times or more of the fluid velocity. Therefore, it is calculated as $P_0 = \frac{10\rho_0 u_{max}}{\gamma}$.

During the squeeze casting process, when the flowing hot fluid contacts the casting mold wall, local overheating may occur, affecting the accuracy of the simulation results. To solve this problem, an artificial heat correction method is adopted to better simulate the heat - exchange process when the hot fluid contacts the wall. Its expression is:

$$H_i = 2\sum_{j=1}^{N}\frac{\bar{q}_{ij}}{\bar{\rho}_{ij}}\frac{e_i - e_j}{|x_{ij}|^2 + \phi^2}x_{ij}\cdot\nabla_i W_{ij}\#(40)$$

where the expressions of the heat terms q_i and q_j are:

$$q_i = \alpha_\Pi h_i p_i c_i\left|\nabla\cdot v_i\right| + \beta_\Pi h_i^2 p_i c_i\left|\nabla\cdot v_i\right|^2\#(41)$$

$$q_j = \alpha_\Pi h_j p_j c_j\left|\nabla\cdot v_j\right| + \beta_\Pi h_j^2 p_j c_j\left|\nabla\cdot v_j\right|^2\#(42)$$

$$\bar{q}_{ij} = q_i + q_j\#(43)$$

3 Case verification and Comparative Analysis of SPH Algorithm

In this paper, the above-mentioned SPH algorithm is used to simulate the squeeze casting of the ZM5 magnesium alloy partition plate for the mine casing (as shown in Figure 2), and the simulation results are compared and analyzed with the simulation results of ProCast. The overall height of this casting is 70 mm, the diameter is 281 mm, the hollow part in the middle is 73 mm, the diameter of the small cylinder at the wall surface is 24 mm, and the length, width and height of the rectangular block at the wall surface are 50 mm, 21.4 mm and 13 mm respectively. The simulation size is the same as the actual size. The material of the casting partition plate part is selected as ZM5 magnesium alloy. This alloy has a simple composition, excellent casting properties and good fluidity. Its solidus temperature is 421 °C and its liquidus temperature is 602 °C. The mold material for the ZM5 magnesium alloy partition plate part is selected as the conventional mold steel H13.

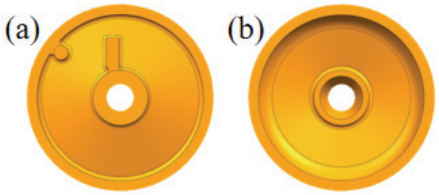

Fig.2: CAD drawing of castings
(a)Convex surface (b)Concave surface

Firstly, an SPH-based squeeze casting mold model is established (as shown in Figure 3). This mold model is composed of the mold, the punch, the molten metal, and the cavity. The materials of the mold and the punch are H13 steel. The mold and the punch are uniformly defined as boundary particles, that is, virtual particles, with a total number of 465,816 particles; the number of ZM5 magnesium alloy molten metal particles is 59,840. The particle spacing is 1.0 mm, and the smoothing length h is 1.5 times the particle spacing, that is, 1.5 mm, and the heat transfer coefficient is set to 2000 W/(m²·K).

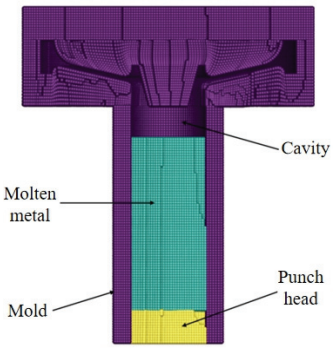

Fig.3: Schematic Diagram of the Squeeze Casting Mold Model

The initial temperature of the molten metal is 720 °C, the initial temperature of the mold is 200 °C, the speed of the punch is set to 0.025 m/s, the moving distance of the punch is 0.7 m, and the mold-filling time is 4.0 s. The mold-filling process is as follows: First, the molten metal is slowly poured into the mold. After the molten metal is poured, the mold is closed. Then, the punch pushes upward to push the molten metal into the cavity, and the mold-filling is completed. A self-programmed SPH-based

three-dimensional program is used to perform a numerical simulation of the ZM5 magnesium alloy partition plate part.During the mold-filling process, the molten metal is pushed upward from the bottom by the punch. When the time is 0.8 s, the molten metal has evenly covered the cylinder and the rectangular parallelepiped on the wall surface, and the viscous liquid can be seen at the edge. Although the shape of the liquid is irregular, it flows smoothly, and the flow direction gradually spreads around. When the time is 1.6 s, the wall surface of the ZM5 magnesium alloy partition plate part has been filled, and the edge part of the ZM5 magnesium alloy partition plate part is about to be filled. At this time, the flow pattern of the molten metal still conforms to the flow law of the molten metal during mold-filling. When the time is 4.0 s, the mold-filling of the ZM5 magnesium alloy partition plate part is completed, as shown in Figure 4(a), (b), (c).

The partition plate part and its gating system are imported into the ProCast software, and then the meshing is carried out. The material parameter settings are consistent with those of the SPH simulation method. After the material parameter settings are completed, the outer surface boundary conditions, interface boundary conditions and interface heat transfer coefficient are set. When t = 0.8s, t = 1.6s, and t = 4.0s, the molten metal flows from the punch into the wall surface of the partition plate part from bottom to top and spreads around until the mold filling is completed, as shown in Figure 4(d), (e), (f).The mold filling process simulated by the ProCAST software is consistent with that simulated by the SPH method, which illustrates the correctness of this model.

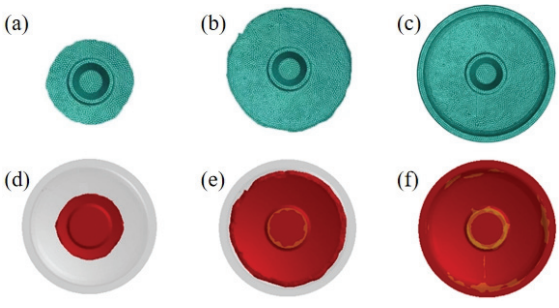

Fig.4: Comparison Diagram of the Flow Field Simulation of the Partition Plate Part by the SPH-based Method and the ProCast Method (a), (d) T = 0.8s (b), (e) T = 1.6s (c), (f) T = 4.0s

4 Conclusions

The meshless method has higher accuracy and stability in dealing with complex boundaries, large deformations, multiphase fluids and free surface problems, and has broad application prospects in the field of casting numerical simulation. In this paper, a simulation casting calculation program based on Smooth particle Fluid Dynamics (SPH) was independently written. The filling process of extrusion casting was numerically simulated and studied. The simulation results were compared and verified with the foreign casting numerical simulation software ProCAST, providing assistance for the SPH method in simulating and predicting the filling of castings and formulating actual production process parameters.

Acknowledgments

National Natural Science Foundation of China (523753945225390, U23A20628, 52305429), Shanxi Provincial Basic Research Program(202301050201004).

Conflicts of interest:

The authors declare that they have no known competing financial interests or personal relationships that could have appeared to influence the work reported in this paper.

References

[1] Liwen, C., Yuhong, Z., Xiaoping, S., et al. Research on the squeeze casting process of ZM5 magnesium alloy partition parts[J]. Special Casting & Nonferrous Alloys, 2023, 43(07): 865-870.

[2] Hailong, J., Mengna, Z., Ming, Y., et al. Research progress of squeeze cast magnesium alloys[J]. Materials China, 2021, 40(10): 772-784.

[3] Jingyi, L., Yuhong, Z., Liwen, C., et al. Numerical simulation of the low-pressure casting process for magnesium alloy partition castings[J]. Special Casting & Nonferrous Alloys, 2021, 41: 588-592.

[4] Hua, H., Yuchun, J., Yuhong, Z., et al. Compiled. Liquid Forming Process and CAD [M]. National Defense Industry Press, 2012.

[5] Yuhong, Z., Xiaofeng, N., Hua, H. Numerical simulation of the temperature field of magnesium alloy squeeze casting based on FDM/FEM [J]. Ordnance Material Science and Engineering, 2011, 34: 1-4.

[6] Hua, H., Hong, X., Jun, C. Research on the application technology of casting CAD/CAE [J]. Foundry, 2003, 52: 1087-1090.

[7] Hua Hou*, Jun Cheng, Hong Xu. Development of CAD software package of intellectualized casting technology [J]. Journal of Central South University of Technology, 12 (2005) 280-283.

[8] Han J ,Du G ,Mi S .A parallel stabilized finite element method for the Navier-Stokes problem[J].Computers and

Mathematics with Applications,2024,17033-41.

[9] Suttakul P ,Vo D ,Fongsamootr T , et al.The role of machine learning for insight into the material behavior of lattices: A surrogate model based on data from finite element simulation[J].Results in Engineering,2024, 23102547-102547.

[10] Hang Z ,Jiale G ,Shuo Z , et al.An effective method for large-scale temperature simulation in SLM based on the finite difference[J].Numerical Heat Transfer, Part A: Applications,2023,83(5):503-521.

[11] Rao, X., He, X. P., Zhao, H., et al. A New Method for Simulating Two - Phase Seepage Streamlines Based on the Mimetic Finite Difference Method [J/OL]. Chinese Journal of Computational Mechanics, 1 - 9[2024 - 09 - 07].

[12] Cen J ,Zou Q .Deep finite volume method for partial differential equations[J].Journal of Computational Physics,2024,517113307-113307.

[13] Gao X ,Li L T ,Qiao W Y , et al.A combined method using Lattice Boltzmann Method (LBM) and Finite Volume Method (FVM) to simulate geothermal reservoirs in Enhanced Geothermal System (EGS)[J].Journal of Groundwater Science and Engineering,2024,12(2):132-146.

[14] Dong L ,Jiaqi P ,Hua H , et al.Optimizing solidification dendrites and process parameters for laser powder bed fusion additive manufacturing of GH3536 superalloy by finite volume and phase-field method[J].Journal of Materials Research and Technology,2023,27 3323-3338.

[15] XU Ruo-zhen, JIANG Yin-fang, MENG Xiang-bao, et al. Numerical simulation research of squeeze casting for vehicle sub-frame[J]. Hot Working Technology, 2016, 45(21): 94−96.

[16] LI Y Z, YANG H B, XING Z W. Numerical simulation and process optimization of squeeze casting process of an automobile control arm[J]. International Journal of Advanced Manufacturing Technology, 2017, 88: 941 − 947.

[17] BABAEE M H, MALEKI A, NIROUMAND B. A novel method to improve interfacial bonding of compound squeeze cast Al/Al-Cu macrocomposite bimetals: Simulation and experimental studies[J]. Transactions of Nonferrous Metals Society of China, 2019, 29(6): 1184.

[18] Chen L, Li J, Zhao Y, et al. Numerical simulation and optimization of indirect squeeze casting process[J]. Engineered Science, 2020, 13(2): 65-70.

[19] Yuwei, C., Yuhong, Z., Xiaolong, P., et al. A Mesh Generation Method for Casting Simulation Based on Boundary Mesh Projection [J/OL]. Special Casting & Nonferrous Alloys, pp. 1-8.

[20] Xiaoyang, X., Wei, Y. Improved Smoothed Particle Hydrodynamics Simulation of Natural Convective Heat Transfer Problems [J/OL]. Chinese Journal of Computational Mechanics, pp. 1-8 [retrieved on 2024-09-07].

[21] Zili, D., Baisen, L., Xiaofeng, L. Simulation of the Movement and Evolution Process of Submarine Landslides Based on the SPH Method [J/OL]. Journal of Engineering Geology, pp. 1-12 [retrieved on 2024-09-07].

[22] Torabbeigi M ,Akbari H ,Adibzade M , et al.Modeling wave dynamics with coastal vegetation using a smoothed particle hydrodynamics porous flow model[J].Ocean Engineering,2024,311(P2):118756-118756.

[23] Lucy L B. A numerical approach to the testing of fission hypothesis[J]. The astronomical journal, 1977, 8(12): 1013-1024.

[24] Gingold R A, Monaghan J J. Smoothed particle hydrodynamics: theory and application to non-spherical stars[J]. Monthly Notices of the Royal Astronomical Society, 1977, 3: 3.

[25] P.W. Cleary, J. HA, V. Alguine, T. Nguyen Flow modelling in casting process Appl. Math. Model., 26 (2002), pp. 171-190.

[26] P.W. Cleary, J. HA, M. Prakash, T. Nguyen 3D SPH flow predictions and validation for high pressure die casting of automotive components Appl. Math. Model., 30 (2006), pp. 1406-1427.

[27] J. Ha, P.W. Cleary Comparison of SPH simulations of high pressure die casting with the experiments and VOF simulations of Schmid and KleinInt. J. Cast Metal Res., 12 (2000), pp. 409-418.

[28] Ha, Joseph, et al. "Simulation of die filling in gravity die casting using SPH and MAGMAsoft." Proc. 2nd Int. Conf. on CFD in Minerals & Process Industries. 1999.

[29] Colagrossi, Andrea, and Maurizio Landrini. "Numerical simulation of interfacial flows by smoothed particle hydrodynamics", Journal of Computational Physics 191.2 (2003): 448-475.

[30] Jinbo, J., Tiancheng, W., Haowei, W., et al. Construction of a Prediction Model for Cold Shut Defects in Die Cast AM60B Magnesium Alloy Based on the SPH Method[J]. Special Casting & Nonferrous Alloys, 2023, 43(07): 967-970.

[31] Mengqing, S., Bingxi, M., Xiaofeng, N. Numerical Simulation Research on Multi-Track Forming of Selective Laser Melting of 316L Stainless Steel[J]. Special Casting & Nonferrous Alloys, 2022, 42(07): 894-897.

[32] Lucy L B .A numerical approach to the testing of the fission hypothesis[J].The Astrophysical Journal, 1977, 8(12):1013-1024.

[33] Gingold R A , Monaghan J J .Smoothed particle hydrodynamics: theory and application to non-spherical stars[J].Monthly Notices of the Royal Astronomical Society(3):375-389[2024-09-07].

[34] Gauss J C F .Theoria Motus Corporum Coelestium in Sectionibus Conicis Solem Ambientium[M]. 2011.

[35] Rudemo, M., Histogram, E. C. O. , & Estimators, K. D. Rosenblatt, M. (1956) \\Remarks on some nonparametric estimates of a density function," Annals of Mathematical Statistics, 27, 832-837.

[36] Epanecnikov V A .Non-parametric estimation of a multivariate probability density[J].Theory of Probability and Its Applications, 1969.

[37] Guirong, L. Smoothed Particle Hydrodynamics [M]. Changsha: Hunan University Press, 2005: 102-165.

[38] Hongfu, Q. New Methods and Applications of Smoothed Particle Hydrodynamics [M]. Beijing: Science Press, 2017: 20 - 35.

[39] Monaghan JJ.On the problem of penetration in particle methods[J]. Journal ofComputational Physics,1989,82 (1):1-15.

[40] Monaghan J J.SPH without a tensile instability.J Camp Phys,2000,159:290~311.